RESEARCH

Synthesis and Neurobehavioral Evaluation of a Potent Multitargeted Inhibitor for the Treatment of Alzheimer's Disease

Mohd Shahnawaz Khan[1] · Zuber Khan[2] · Nasimudeen R. Jabir[3] · Sidharth Mehan[2] · Mohd Suhail[4,5] ·
Syed Kashif Zaidi[6] · Torki A. Zughaibi[4,5] · Mohammad Abid[7] · Shams Tabrez[4,5]

Abstract

Alzheimer's disease (AD) poses a significant health challenge worldwide, affecting millions of individuals, and projected to increase further as the global population ages. Current pharmacological interventions primarily target acetylcholine deficiency and amyloid plaque formation, but offer limited efficacy and are often associated with adverse effects. Given the multifactorial nature of AD, there is a critical need for novel therapeutic approaches that simultaneously target multiple pathological pathways. Targeting key enzymes involved in AD pathophysiology, such as acetylcholinesterase, butyrylcholinesterase, beta-site APP cleaving enzyme 1 (BACE1), and gamma-secretase, is a potential strategy to mitigate disease progression. To this end, our research group has conducted comprehensive in silico screening to identify some lead compounds, including IQ6 (SSZ), capable of simultaneously inhibiting the enzymes mentioned above. Building upon this foundation, we synthesized SSZ, a novel multitargeted ligand/inhibitor to address various pathological mechanisms underlying AD. Chemically, SSZ exhibits pharmacological properties conducive to AD treatment, featuring pyrrolopyridine and N-cyclohexyl groups. Preclinical experimental evaluation of SSZ in AD rat model showed promising results, with notable improvements in behavioral and cognitive parameters. Specifically, SSZ treatment enhanced locomotor activity, ameliorated gait abnormalities, and improved cognitive function compared to untreated AD rats. Furthermore, brain morphological analysis demonstrated the neuroprotective effects of SSZ, attenuating Aβ-induced neuronal damage and preserving brain morphology. Combined treatment of SSZ and conventional drugs (DON and MEM) showed synergistic effects, suggesting a potential therapeutic strategy for AD management. Overall, our study highlights the efficacy of multitargeted ligands like SSZ in combating AD by addressing the complex etiology of the disease. Further research is needed to elucidate the full therapeutic potential of SSZ and the exploration of similar compounds in clinical settings, offering hope for an effective AD treatment in the future.

Keywords Alzheimer's disease · Beta-amyloid · Neurodegeneration · Neuroprotection · SSZ

Abbreviations

AchE	Acetylcholinestrase
AD	Alzheimer's disease
Aβ	Amyloid-beta
Bax	Bcl-2-associated X protein
DON	Donepezil
ELT	Escape latency time
GSH	Reduced glutathione
LDH	Lactate dehydrogenase
MAP	Myelin associated proteins
MBP	Myelin basic protein
MD	Malondialdehyde
MEM	Memantine
NEFL	Neurofilament light chain
NMDA	N-Methyl-d aspartate
No	Nitric oxide
SOD	Superoxide dismutase
SSZ	6-chloro-N-cyclohexyl-4-(1Hpyrollo[2,3-b] pyridin-3-yl] pyridin-2-amine
TSTQ	Time spent in the target quadrant
LA	Locomotor activity
MWM	Morris water maze
BCT	Beam-crossing task

The authors Mohd Shahnawaz Khan and Zuber Khan contributed equally.

Extended author information available on the last page of the article

Introduction

Alzheimer's disease (AD) is a progressive cognitive decline that accounts for 70% of dementia cases and remains a significant health concern, especially in the elderly population. A recent report suggested that globally, around 50 million people are affected with dementia, ranking as the sixth most prevalent cause of mortality [1]. AD is expected to impact around 152 million people by 2050 as the global population ages. The likelihood of this disease is further exacerbated by the rising incidence of various other risk factors, such as depression, smoking, diabetes, obesity, and hypertension [2, 3]. Instantaneous measures are required to prevent the long-term epidemiological trends of AD, avoid the onset, delay progression, or improve symptoms of AD.

Clinically, AD has been generally manifested as a progressive neuronal atrophy resulting in a memory decline, problems with communication, space disorientation, and many more [2, 4]. The etiology of AD is primarily explained by disrupted neurotransmitter systems, atypical β-amyloid and tau protein deposition, oxidative stress, mitochondrial dysfunction, synaptic loss, and neuronal cell death [5, 6]. Despite the great effort of contemporary pharmacological management, the restoration of neuronal degeneration in AD offers little success, which is often associated with severe side effects, resulting in an increased death risk [7–9]. Frequently cited reasons for pursuing this treatment gap entail the disease's complexity and multifactorial non-specific etiologies [10, 11].

Currently, the treatments for AD mainly focus on addressing the acetylcholine deficiency by targeting the cholinesterase enzymes as a drug target. Cholinesterase inhibitors (donepezil, galantamine, and rivastigmine) have been accepted as the first-line symptomatic pharmacologic treatment for patients with mild-to-moderate AD [12, 13]. Similarly, managing Aβ plaques in the brain by inhibiting the beta-site amyloid precursor protein cleaving (BACE-1) enzyme also holds an effective strategy [14]. However, the current approaches are inadequate, costly, and provide only symptomatic treatment. Due to the involvement of different mechanistic pathways, simultaneous blockage of multiple targets should be the therapeutic strategy that might lead to the desired outcome against AD [15–17].

We have pursued this approach for years to develop a viable multitargeted medicament for treating AD. Our research group completed a comprehensive in silico screening and reported several potential lead compounds that could target multiple enzymes, viz. acetylcholinesterase, butyrylcholinesterase, glycogen synthase kinase 3, BACE-1, and gamma-secretase, and possibly provide a successful anti-AD drug [18–20]. From computational studies, we obtained 48 ligands that showed absolute binding energy < − 8 kcal/mol. Among those, 13 ligands (BRW, 6VK, 6Z5, SMH, X37, 55E, 65 A, IQ6, 6VL, 6VM, F1B, 6Z2, and GVP) were selected based on blood–brain barrier (BBB) permeability, acceptable ADME properties as well as their molecular interaction profiles with the target enzymes [20]. Out of those 13 ligands, eight ligands (55E, 6Z2, 6Z5, BRW, F1B, GVP, IQ6, and X37) showed the binding energies of ≤ − 8.0 kcal/mol towards BChE, BACE-1, gamma-secretase, MAO-A, and MAO-B, and formed a stable complex with target enzymes. The rationale behind selecting the lead compound IQ6 was a comparative ease of synthesis, cost-effectiveness, and it also contains both N-cyclohexyl and pyrrolopyridine groups that have shown anti-AD effects in previous studies [21–23]. It was also a matter of further investigation to check the potential efficacy of our IQ6 compound in animal models.

Chemically, IQ6 is 6-chloro-N-cyclohexyl-4-(1Hpyrollo[2,3-b] pyridin-3-yl] pyridin-2-amine with viable pharmacological properties. Pyrrolopyridine scaffolds are often found in naturally occurring polyheterocyclic compounds that contain pyrrole and pyridine as active pharmacophores and have been the focus of several drug discoveries [24, 25]. Pyrrolopyridine-containing compounds have a long history of pharmacological actions, including antiviral, anticancer, and antimicrobial effects [26–28]. Pyrrolo[2,3-b]pyridine found in the ligand IQ6 is one of the six structural isomers of pyrrolopyridine, a heterocyclic molecule having a five-membered pyrrole ring fused to a six-membered pyridine ring [24]. This compound derivative has also been reported as a structural moiety in multiple anti-AD drug targets, such as phosphodiesterase and monoamine oxidase B [29, 30]. Similarly, N-cyclohexyl fragments are often applied as constituents in synthetic and natural drugs, where they can function as the primary structural element or as a side chain. It has also been reported as a functional element for inhibitory actions against multiple targets, such as BACE1 and butyrylcholinesterase [21]. In contrast to the previously published findings, the scaffolds presented here are believed to have enhanced pharmacological properties, significantly improving efficacy against AD.

Material and Methods

Chemicals and Drugs

IQ6 (SSZ) was synthesized using the method reported in the literature [31]. The chemical shift values of ^{1}H NMR were reported in parts per million (ppm) relative to residual solvent (DMSO-d_6, δ 2.50 ppm), and ^{13}C NMR chemical shifts (δ) of ^{13}C NMR were reported in ppm relative to (DMSO-d_6, δ 39.52 ppm) and Hertz (Hz) is the unit of coupling constants (J). Agilent G6530AA (LC-HRMS-Q-TOF) spectrometer was used to record mass spectra. Intraperitoneal administration of SSZ took place after its dissolution in 1% dimethyl sulfoxide (DMSO) following established protocols [32–34]. Neurotoxin amyloid beta (Aβ) was procured from Sigma-Aldrich (USA). On the other hand, memantine (MEM) and donepezil (DON) were obtained from Sun Pharma, New Delhi, India. These drugs were administered intraperitoneally (i.p.) after they dissolved in 1% DMSO as per the previously described methods [35, 36]. It is critical to acknowledge that thorough preparation was conducted before administering all the substances and medications during the experiment, thereby guaranteeing the credibility and dependability of the study's results.
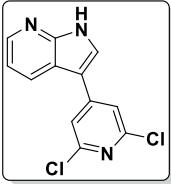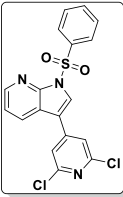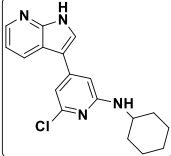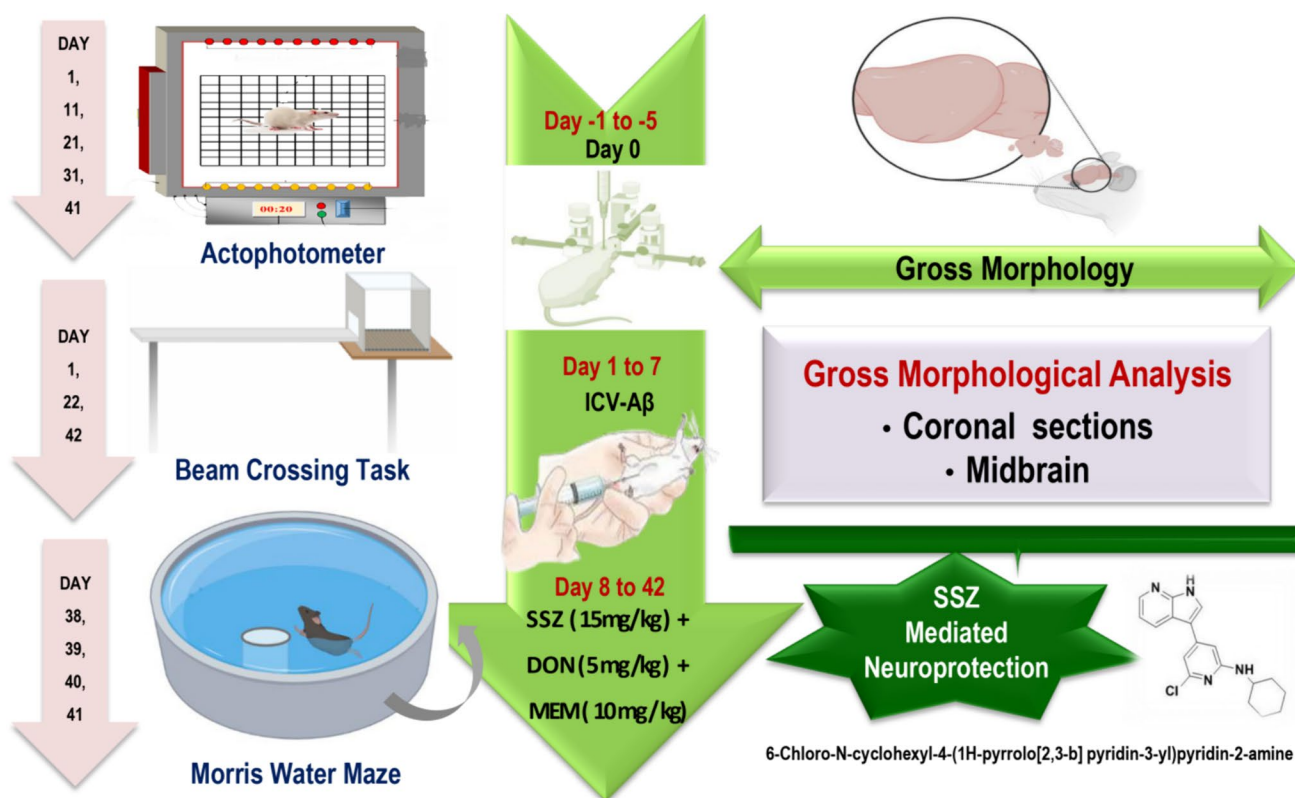

Fig. 1 Experimental protocol schedule

Step I: *Synthesis of 3-(2,6-dichloropyridin-4-yl)-1-phenylsulfonyl)-1H-pyrrolo[2,3-b]pyridine*(**3**) To a suspension of 1-(phenylsulfonyl)-3-(4,4 5,5-tetramethyl-1,3,2-dioxaborolan-2-yl)-1H-Pyrrolo 2.3-b]pyridine (1) (1.0 equiv) 2,6-dichloro-4-iodopyridine (**2**) (1.2 eq) in 1,2-dimethoxyethane/ethanol/water (7:2:3) was added sodium carbonate (2.5 eq) degassed with nitrogen balloon for 20-30 minutes. To the above suspension was added Dichlorobis(triphenylphosphine palladium(II) (0.1 eq), and finally degassed and heated at 80°C overnight. The reaction mixture was cooled and filtered, and the filtrate was diluted with ethyl acetate and washed with water. The organic layers were washed with brine, dried over anhydrous Na_2SO_4, filtered, and concentrated under *a vacu*um. The crude was purified by column chromatography over 100-200 silica gel, and the product was eluted with ethyl acetate-hexane (2:8) to yield the title compound (**3**).	
Step II: *Synthesis of 3-(2,6-dichloropyridin-4-yl)-1H-pyrrolo[2.3-b]pyridine* (**4**) To a solution of 3-(2,6-dichloropyridin-4-yl)-1-phenylsulfonyl)-1H-pyrrolo[2,3-b]pyridine (1.0 eq) in ethanol/water (5/1) was added powdered KOH (6.0 eq). The resulting solution was heated at 40 °C for 24 hours. After the reaction, most of the solvent was removed *in vacuo*, and the residue was diluted with ethyl acetate and washed with water brine. The organic layer was dried over anhydrous Na2SO4, filtered, and concentrated. The crude was purified by column chromatography over 100-200 silica gel and eluted with ethyl acetate-hexane (3:7) to yield the pure product compound (**4**).	
Step III: *Synthesis of 6-chloro-N-cyclohexyl-4-(1H-pyrrolo[2,3-b]pyridin-3-yl)pyridin-2-amine* (**6**) A mixture of 3-(2,6-dichloropyridin-4-yl)-1H-pyrrolo[2,3-b]pyridine(**4**) (1.0 eq) and cyclohexylamine (**5**) (1.5 eq) in DMF (2mL/mmol) was heated in a sealed tube at 150°C for 20 h. The reaction was cooled, poured into ice-cold water, and extracted with ethyl acetate (3x20 mL). The combined organic layer was washed with water and brine and dried over anhydrous Na_2SO_4. The organic layer was concentrated, and the crude residual oil was purified by flash chromatography on silica gel eluting with 10-20% ethyl acetate in hexanes to provide the title compound (**6**) **as** light brown solid.	

6-chloro-N-cyclohexyl-4-(1H-pyrrolo[2,3-b] pyridin-3-yl) pyridin-2-amine

Brown solid; yield 78%; $R_f = 0.32$ (ethyl acetate: hexane); FT-IR (cm^{-1}): 3084, 3032, 9224, 2852, 2343, 2111, 1655, 1589, 1522, 1396, 1281, 1258, 1122; ^{1}H NMR (400 MHz, DMSO-d_6) (δ, ppm): 12.19 (s, 1H, N–H $_{pyrrole}$), 8.34 (d, $J = 7.99$ Hz, 1H, Ar–H), 8.31 (d, $J = 4.59$ Hz, 1H, Ar–H), 8.19 (d, $J = 2.33$ Hz, 1H, Ar–H), 7.92 (s, 1H, Ar–H), 7.22–7.18 (m, 1H, Ar–H), 6.96 (s, 1H, Ar–H), 6.82 (s, 1H, N–H), 3.63–3.56 (m, 1H, C–$H_{cyclohexyl ring}$), 1.73–1.14 (m, 10H, C–$H_{cyclohexyl ring}$); ^{13}C NMR (100 MHz, DMSO-d_6) (δ, ppm): 160.42, 159.84, 149.41, 146.93, 143.76, 131.99, 128.31, 127.06, 117.15, 112.06, 107.74, 100.73, 46.72, 38.25, 32.80, 25.70, 24.94; HRMS (m/z) calcd. For $C_{18}H_{19}ClN_4$: 326.1298 Found: 327.1376 [M + H]$^+$.

Animals

We used 56 adult Wistar rats, with an equal distribution of 28 males and 28 females, as experimental subjects. Rats weighing 200–250 g were obtained from the ISF College of Pharmacy's Central Animal House in Moga, Punjab, India. To maintain constant living conditions, we individually confined the animals in polyacrylic cages measuring 38 cm × 32 cm × 16 cm. Each cage housed two rats and provided comfortable bedding. The husbandry practices adhered to established norms, giving ad libitum access to water and food. Strict regulation of environmental parameters ensured a humidity of $55 \pm 10\%$, an average temperature condition of 22.2 ± 2 °C, and automated lighting that facilitated a 24-h cycle of the organism. Before the initiation of experimental procedures, a 5-day acclimation period was instituted to allow the rats to acclimatize to their surroundings.

Animal Ethical Approval

Registration number 816/PO/ReBiBt/S/04/CPCSEA indicates that the Institutional Animal Ethics Committee (IAEC) has approved the experimental protocol in accordance with the regulations established by the government of India. The IAEC meticulously reviewed ISFCP/IAEC/CPCSEA/Meeting number 03/2022/Protocol number 21 to ensure adherence to the ethical standards and regulations of the Committee for the Purposes of Control and Supervision of Experiments on Animals (CPCSEA). The approval signifies adherence to established regulatory frameworks and attests to the ethical and methodological soundness of the proposed research endeavor.

Experimental Animal Classification

The experimental design employed a randomized allocation process to assign participants to seven distinct groups, as follows: group 1 received a sham control intervention; group 2 underwent a vehicle control treatment; group 3 was treated with SSZ Perse at a dosage of 15 mg/kg administered intraperitoneally (i.p.); group 4 was exposed to Aβ (200 ng/5 μL) through intracerebroventricular (ICV) administration; group 5 received a combined treatment of Aβ (200 ng/5 μL, ICV) and SSZ (15 mg/kg, i.p.); group 6 was subjected to Aβ (200 ng/5 μL, ICV) along with SSZ 15 mg/kg., i.p. and DON at a dose of 5 mg/kg, i.p.; and finally, group 7 was administered Aβ (200 ng/5 μL, ICV) in conjunction with SSZ 15 mg/kg., i.p., and MEM at a dose of 10 mg/kg, i.p. This comprehensive grouping strategy aimed to systematically investigate and compare the effects of these various interventions on the experimental outcomes.

Experimental Procedure Schedule

Experimental research spanned a total of 42 days, meticulously designed to minimize the impact of circadian rhythms by confining activities to the time frame of 9:00 a.m. to 2:00 p.m. AD induction in experimental rats involved ICV administration of Aβ from days 1 to 5. From the 6th to the 42nd day, we intraperitoneally administered SSZ at a 15 mg/kg dosage. To evaluate the efficacy of SSZ treatment, concurrent intraperitoneal administration of the acetylcholinesterase inhibitor donepezil (DON) at a dose of 5 mg/kg and the NMDA receptor blocker memantine (MEM) at 10 mg/kg was given between days 6 and 42. During the 42-day experiment, we used an actophotometer to measure the rats' LA, ran trials in the Morris water maze (MWM), gave them the beam crossing task (BCT), and checked their variation in body weight to look into the phenotypic manifestations of AD.

After completing the experimental regimen on day 42, we anesthetized the animals and sacrificed them on day 43. We extracted and meticulously preserved the intact brains in formalin. Biochemical analysis and gross pathological changes examination were performed on these brain specimens in order to identify any white matter fiber reductions within the brain. Figure 1 presents an illustrative depiction of the experimental approach, as referenced in the works of [32–34, 37].

Methods

Animal Model for AD Induced by Amyloid-β Administration

Before the experimentation study, the rodents adapted to the laboratory's environmental surroundings. Following

this, we injected 75 mg/kg of ketamine intraperitoneally to anesthetize the animals. Once the rodents were anesthetized, we carefully placed each rat on a warm pad held within a stereotaxic apparatus (Stoelting Co., Wood Dale, IL, USA) in order to immobilize their heads. We cleansed the scalp with 70% ethanol, shaved it, and made the incision through the mid-sagittal plane of the rodent head. The exposed skull allowed for the identification of the bregma and lambda, aiding in determining the coordinates for ICV injection and controlling bleeding using saline-soaked cotton swabs. The right lateral cerebral ventricle was accessed by a drilled hole through the parietal bone, with stereotaxic coordinates of VP-3.0 mm from the skull surface, ML ± 1.5 mm from the mid-sagittal suture, and AP-0.92 mm from the bregma region [38, 39]. Through the small incision, a 2.5-cm cannula was placed and sealed with the help of a plastic earpin. After securing the aperture with dental cement, a readily absorbable surgical ligature was used to close the opening. Using a 10-µL Hamilton microliter syringe coupled to a hypodermic needle (0.4 mm external diameter) at a rate of 5 µL/min, we delivered 5 µL of Aβ (200 ng/body weight), dissolved in 0.1 M citrate buffer at pH 4.5, into the right lateral cerebral ventricle on the first day [34, 40, 41]. The micro-needle remained in place for 5 min after injection to facilitate drug diffusion in the cerebrospinal fluid (CSF). Forty-eight hours later, we repeated the administration of Aβ in the remaining lateral ventricle.

Cannula Implantation

In the experimental protocol, all animals within the study's test groups underwent anesthesia using ketamine (80 mg/kg, i.p.). We carefully performed a midline incision, measuring 1 cm, on the scalp, commencing midway between the eyes and concluding behind the lambda. Next, we meticulously cleared away the soft tissue covering the skull using a cotton swab. A Hamilton syringe, mounted onto an injection pump, was utilized to administer the intracerebroventricular injection (ICV) of amyloid peptide Aβ (1–42) at a dosage of 200 ng/5 µL unilaterally. The needle was arranged strategically, precisely over the bregma, at coordinates AP = 0.92 mm, ML = 1.5 mm, and VP = 3.9 mm in relation to the right side. Next, we drilled a small cranial burr hole through the skull at the designated entry point. We carefully inserted 5 µL of amyloid peptide Aβ (1–42) into the Hamilton syringe, followed by injection at the specified coordinates. After sealing the burr hole with dental cement, the outer skin was sutured to ensure closure. To establish a control group, we injected sham rats with an equivalent volume of saline, following established methodologies reported earlier [32, 33, 42–44].

Post-surgical Treatment

Operative individual rats were kept in warm cloth-lined polyacrylic cages with the husk removed. Until the rats regained spontaneous movement, particular care was given for 2–3 h after anesthesia [45–47]. Postoperative care involved providing milk and glucose water in the cages for 2 to 3 days to mitigate potential physical damage. We also administered gentamicin (35 mg/kg intraperitoneal) to rodents three times daily for 3 days to proactively inhibit the onset of sepsis. Concurrently, we applied Neosporin powder to prevent bacterial skin infections and employed lignocaine gel for pain management in the sutured region. Routinely, we observed clinical indicators such as general body condition and dehydration following surgery. After 7 days, the rats resumed spontaneous movement and ate a healthy meal and water, exhibiting signs of recovery [43, 48–50].

Neurobehavioral Experiments

Locomotor Activity

Using an actophotometer (Swastika, India), we measured the rats' LA. On days 1, 11, 21, 31, and 41 of the trial, we recorded the mice's spontaneous LA after placing every participant in the exact middle of the cubicle. The automated actophotometer methodically recorded the locomotor reactions of the animals during 5-min sessions. We used the counts per 5 min generated from these sessions as a quantitative metric of movement, which allowed a thorough assessment of the animals' natural locomotor behaviors at the given intervals and shed light on their activity patterns during the course of experiment [51].

Beam-Crossing Task (BCT)

The beam-crossing test, devised by the Inco Group of Companies in Ambala, India, constitutes a systematic instrument employed to quantitatively assess animals' susceptibility to elevated stress and its impact on their motor coordination. The experimental chronology included thoroughly evaluating each participant on days 1, 22, and 42. This evaluation included tests of neuromuscular coordination, abnormal locomotion, and foot slippage. The effect of height-induced stress on the motor abilities of the rats was quantitatively evaluated by keeping track of the number of foot slips shown by each rat at 2-min intervals during each session [38, 52, 53].

Body Weight

As any medical illness progresses, a loss in body mass is the primary clinical sign or diagnostic indicator. In this investigation,

researchers used rats as model organisms and measured the participants' body weights on days 1, 7, 14, 21, 28, 35, and 41 to track this physiological parameter [38, 54–56].

Spatial Navigation Task (SNT)

We employed the SNT as a methodological tool to assess the cognitive abilities of experimental animals in terms of their spatial memory and learning proficiency within novel environments. This test was especially noteworthy because it correlated with hippocampal synaptic plasticity and cognitive dysfunction. We carefully monitored rats' escape latency time (ELT) during several testing sessions as they were allowed access to a swimming arena. During the memory consolidation assessment conducted on the 42nd day, rodents had 120 s to discern the location of a relocated platform. Furthermore, we quantified the duration of occupancy within the designated target quadrant (TSTQ) as a metric to gauge the extent of comparative memory consolidation [32, 38, 52].

Gross Pathological Analysis

Following the completion of treatment, the animals were euthanized via intraperitoneal injection of 270 mg/mL sodium phenobarbital. Subsequently, the brains were sensibly extracted from the skulls and preserved in a saline solution that was normal to freezing temperatures. We utilized a digital imaging device to capture video imagery of the entire brain, including all coronal sections, to conduct a comprehensive macroscopic gross pathological examination.

The investigation focused on the grayish areas around the coronal sections, and for each brain segment, the demyelinated volumes (measured in mm^3) were computed. The demyelination volume of each coronal segment was determined by applying the formula (length × breadth × height) to quantify the extent of white matter degeneration. It was possible to evaluate the experimental results accurately thanks to this systematic approach, which showed how the protocol changed the patterns of demyelination in the brain areas studied [38, 44, 52, 57].

Statistical Analysis

We performed a comprehensive statistical analysis on recorded results from several trials using GraphPad Prism 8.0.1 (San Diego, CA, USA). To identify differences in neurobehavioral assessments between treatment groups, we conducted a post hoc Bonferroni test following a two-way analysis of variance (ANOVA). TSTQ parameter was evaluated using a one-way analysis of variance (ANOVA) with repeated measures and Tukey's post hoc test for multiple comparisons. We visually represented the experimental data as mean values and corresponding standard deviations (SD).

At the probability level of $p < 0.05$, the significance criteria were established for interpreting the data.

Results

Chemistry

Suzuki–Miyaura cross-coupling reaction was performed using commercially available 1-(phenylsulfonyl)-3-(4,4 5,5-tetramethyl-1,3,2-dioxaborolan-2-yl)-1H-pyrrolo 2.3-b]pyridine (**1**) and 2,6-dichloro-4-iodopyridine (**2**) in the presence of sodium carbonate and bis(triphenyl phosphene) Pd(II) chloride [(PPh$_3$)$_2$Pd(II)Cl$_2$] to get compound **3**. Hydrolysis of sulfonamide (**3**) was carried out under heating conditions using potassium hydroxide (KOH) in ethanol–water mixture to afford compound **4**. Substitution reaction was done using cyclohexylamine (**5**) under sealed tube condition at a slightly higher temperature (150 °C) in anhydrous N,N-dimethyl formamide (DMF) throughout 24 h to get the final compound **6**. The spectral data for the synthesized compound has also been provided as supplementary file (1) (Scheme 1).

Effect of SSZ Compound on Behavioral Dysfunctions in Aβ-Induced Alzheimer's Rats

Effect of SSZ Compound on Locomotion

The actophotometer was used to measure spontaneous movement at intervals of 10 days throughout the study. Initially, no notable differences were observed among the groups. However, by day 11, rats with AD induced by Aβ showed distinct movement patterns compared to the control groups. By day 21, rats receiving SSZ 15 mg/kg displayed improved locomotion compared to those induced with Aβ. Notably, on days 31 and 41, a combination of SSZ 15 mg/kg with DON 5 mg/kg and MEM 10 mg/kg showed superior performance over individual treatments (two-way ANOVA: $F_{(6, 49)} = 3992$, $p < 0.05$). Specifically, on day 31, SSZ 15 mg/kg combined with DON 5 mg/kg demonstrated more significant activity compared to SSZ 15 mg/kg alone. By day 41, the Aβ, DON 5 mg/kg, and MEM 10 mg/kg groups exhibited increased locomotor behavior, with MEM 10 mg/kg showing a notable enhancement over DON 5 mg/kg alone (Fig. 2).

Effect of SSZ Compound on Neuromuscular Coordination

Rats underwent walking trials on specified days (1, 22, and 42) per the experiment's design to evaluate their
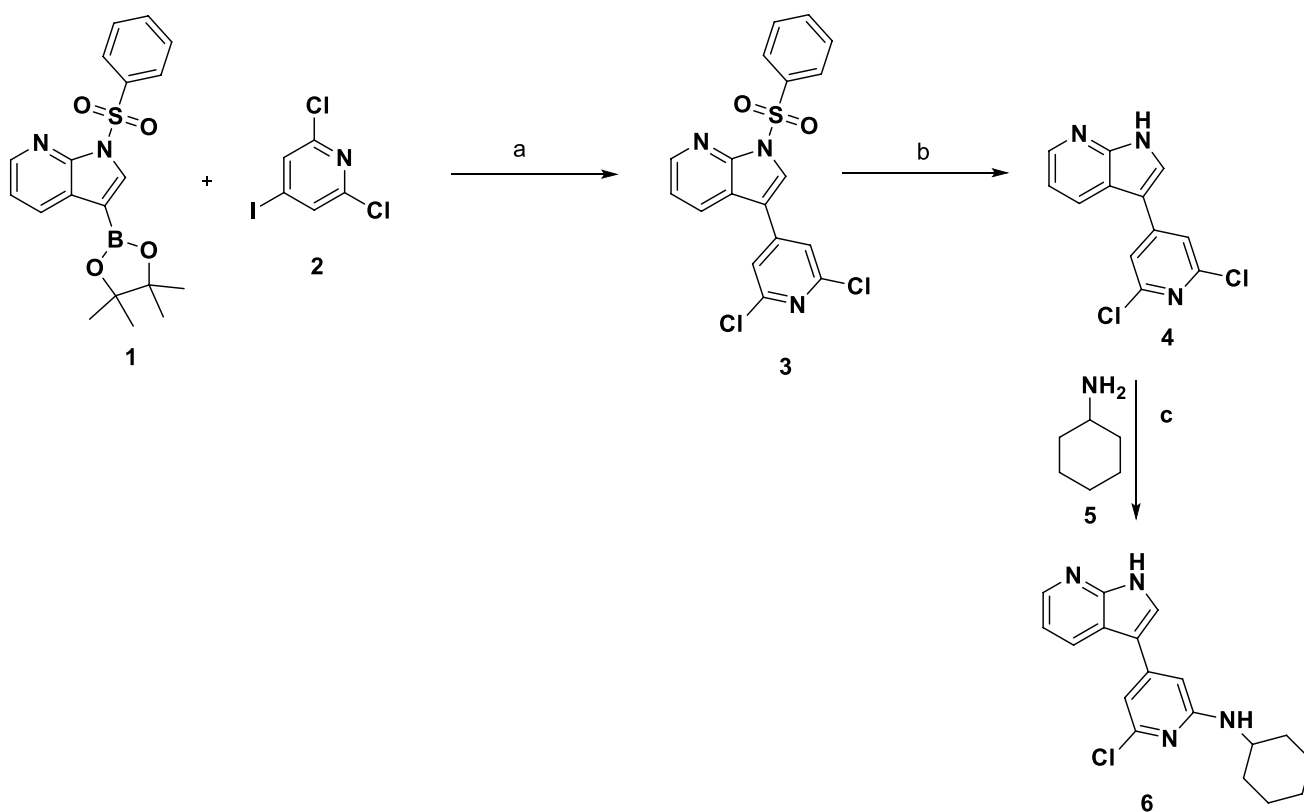
Scheme 1 Reagents and conditions: (**a**) Pd(PPh3)$_2$Cl$_2$, Na$_2$CO$_3$, 80 °C for overnight. (**b**) KOH, 40 °C for 2 h. (**c**) Microwave at 150 °C for 30 min
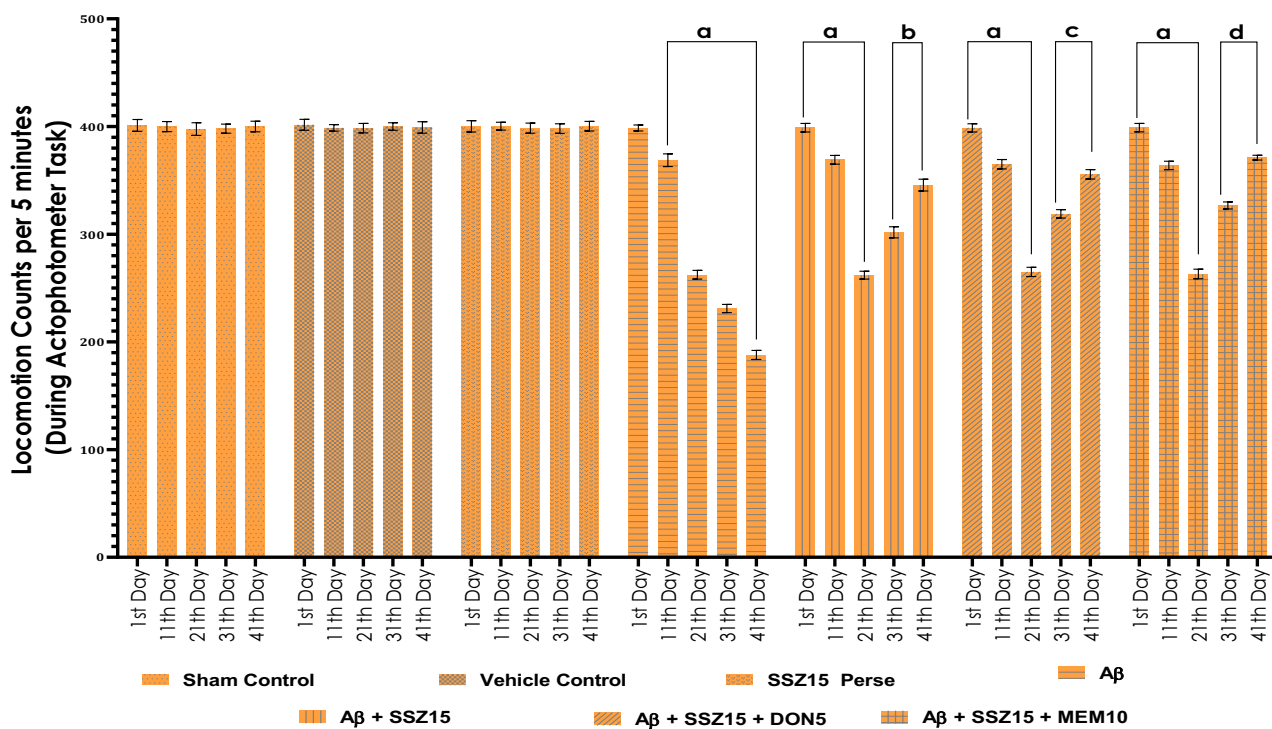

Fig. 2 Effect of SSZ compound on locomotion in Aβ-induced Alzheimer's rats. The statistical assessment used a two-way ANOVA and post hoc Bonferroni testing to analyze the data. Results are represented as mean values with standard deviation ($p < 0.05$), with each experimental group comprising eight Wistar rats. Statistical comparisons were made between groups: (**a**) versus sham control, vehicle control, and SSZ15 perse; (**b**) versus Aβ; (**c**) versus Aβ and SSZ15; and (**d**) versus Aβ, SSZ15, and DON5

coordination and slip occurrences on a BCT surface. Initially, no discernible differences were observed among the treatment groups. However, by day 22, when assessing the impact of Aβ, a notable increase in falls was noted in AD rats treated with Aβ compared to the sham control, vehicle control, and SSZ perse-treated groups (two-way ANOVA: $F_{(6, 49)} = 389.4$, $p < 0.05$). Throughout the study, slip occurrences decreased on days 22 and 42 in the treatment groups compared to the Aβ-treated group. Specifically, on day 22, there was no significant reduction in slip occurrences in the treatment group administered SSZ15 along with the standard drug DON5 compared to the SSZ15 group. However, by day 42, the MEM10 treatment group exhibited significantly fewer slips than the other groups (Fig. 3).

Effect of SSZ Compound on Body Weight Variations

Comparisons were made regarding the weight fluctuations among seven distinct groups at specific intervals throughout the investigation. Initially, no noteworthy variations in weight were observed among these groups. However, by the 7th day, it became evident that rats treated with Aβ displayed a noticeable decrease in weight compared to rats in the sham control, vehicle control, and SSZ-perse treated groups. Over

the subsequent days (7, 14, and 21), the Aβ-treated group consistently exhibited a progressive decrease in body weight relative to the sham, vehicle control, and SSZ Perse groups. Yet, from day 28 onwards, the continuous intraperitoneal administration of SSZ15, in addition to SSZ15 with DON5 and MEM10mg/kg standard drugs, notably and incrementally increased body weight compared to Aβ-induced rats (two-way ANOVA: $F_{(6, 49)} = 987.9$, $p < 0.05$). Notably, the group receiving DON5 and MEM10 experienced a more significant weight increase than the Aβ group. By day 41, the rats treated with SSZ15mg/kg had effectively regained body mass compared to Aβ-treated rats. Additionally, Aβ-induced rats administered SSZ15 mg/kg in combination with MEM10mg/kg recovered substantially more weight than those treated with DON5mg/kg (Fig. 4).

Effect of SSZ Compound on Memory

To evaluate the memory and cognition of experimental rats, their escape latency time (ELT) and time spent in the target quadrant (TSTQ) were measured from days 38 to 41. The rats' time to find the escape route (ELT) and the duration spent in the targeted quadrant (TSTQ) were measured between days 38 and 41 using the Morris water maze test. An evident contrast in ELT was noticed between the
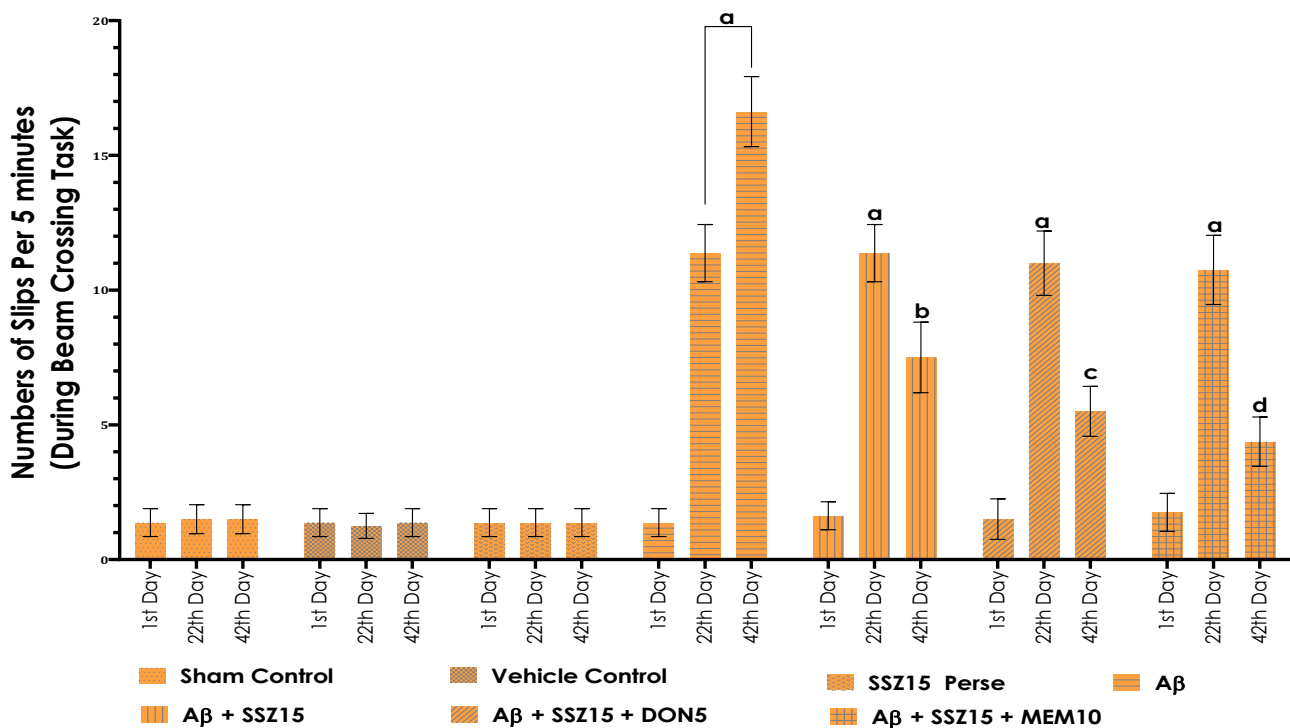

Fig. 3 Effect of SSZ compound on neuromuscular coordination in Aβ-induced Alzheimer's rats. The statistical assessment used a two-way ANOVA and post hoc Bonferroni testing to analyze the data. Results are represented as mean values with standard deviation ($p < 0.05$), with each experimental group comprising eight Wistar rats. Statistical comparisons were made between groups: (**a**) versus sham control, vehicle control, and SSZ15 perse; (**b**) versus Aβ; (**c**) versus Aβ and SSZ15; and (**d**) versus Aβ, SSZ15, and DON5
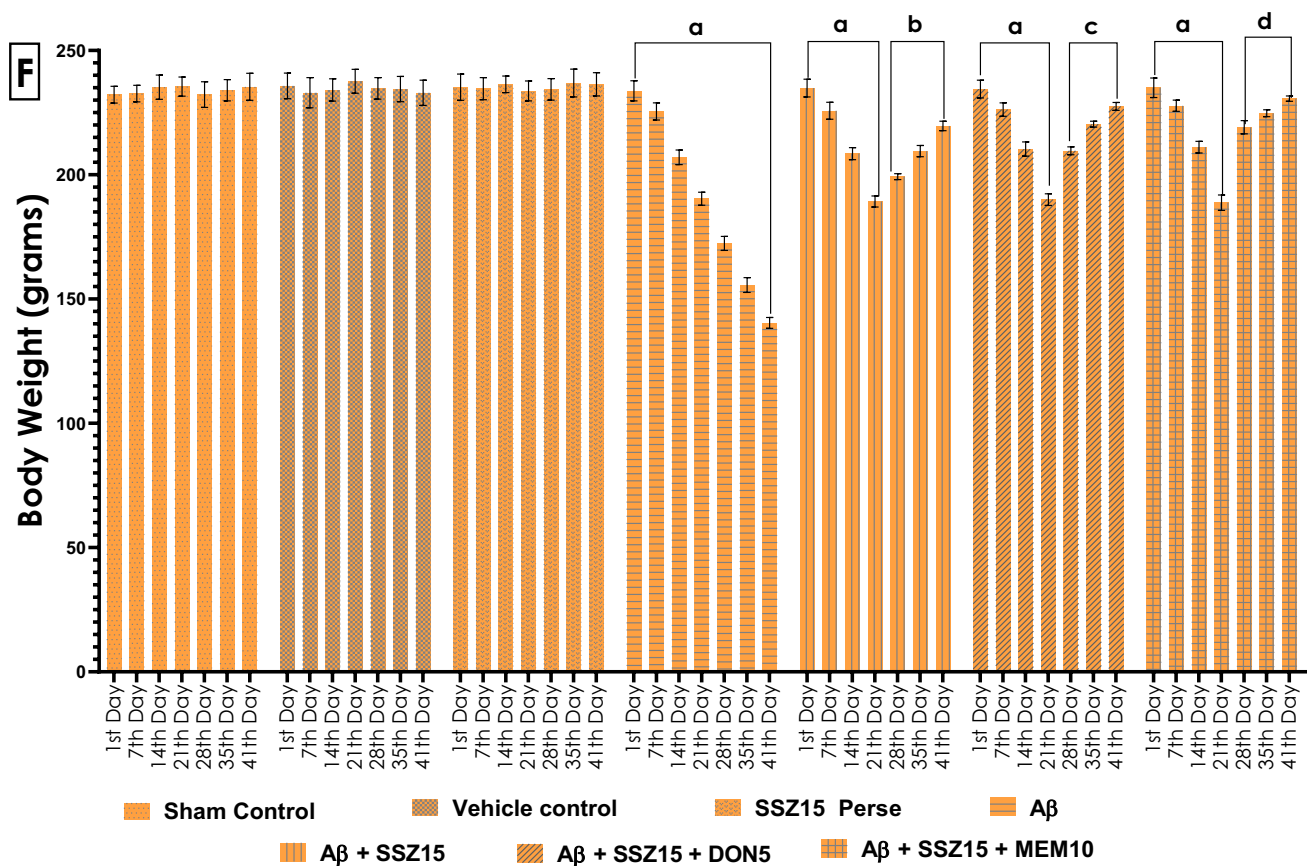
Fig. 4 Effect of SSZ compound on body weight variations in Aβ-induced Alzheimer's rats. The statistical assessment used a two-way ANOVA and post hoc Bonferroni testing to analyze the data. Results are represented as mean values with standard deviation ($p < 0.05$), with each experimental group comprising eight Wistar rats. Statistical comparisons were made between groups: (**a**) versus sham control, vehicle control, and SSZ15 perse; (**b**) versus Aβ; (**c**) versus Aβ and SSZ15; and (**d**) versus Aβ, SSZ15, and DON5

Aβ-induced group and the sham control, vehicle control, and SSZ perse groups, indicating a significant increase in the Aβ-induced group. Moreover, the administration of SSZ at 15 mg/kg illustrated a decrease in ELT compared to Aβ-induced rats. (Analysis revealed significant differences via two-way ANOVA: $F_{(6, 49)} = 7623$, $p < 0.05$).) Furthermore, the MEM10 group displayed a notable reduction in escape latency compared to the Aβ group. Observations on day 41 revealed that rats treated with Aβ, SSZ15, and MEM10 exhibited marginally shorter escape latency compared to those treated with Aβ, Aβ, and DON5 (Fig. 5).

Effect of SSZ Compound on TSTQ

On the 35th day of the investigation, we assessed the duration spent by subjects in the designated quadrant to measure memory consolidation post-treatment in rats. The group induced with Aβ spent less time in this quadrant than the sham control, vehicle control, and SSZ perse groups. Administering SSZ at a dosage of 15 mg/kg via

intraperitoneal injection over an extended period notably increased the time spent in the target quadrant compared to the Aβ-induced group (one-way ANOVA: $F_{(6, 49)} = 799.6$, $p < 0.05$). Additionally, administering DON significantly reduced the time spent in the quadrant in experimental Alzheimer's rats relative to the Aβ rats. We introduced the NMDA antagonist MEM at a dose of 10 mg/kg alongside Aβ, SSZ15, and DON5 to evaluate treatment efficacy. This revealed increased time spent in the target quadrant compared to the Aβ, Aβ, SSZ15, and DON5 groups (Fig. 6).

Effect of SSZ Compound on Gross Morphological Dysfunctions (Coronal Sections) in Aβ-Induced Alzheimer's Rats

Following the completion of the 42-day experimental protocol, adult Wistar rats were euthanized. Subsequently, fresh, intact brains were carefully removed and dissected. These fresh brains underwent coronal sectioning,
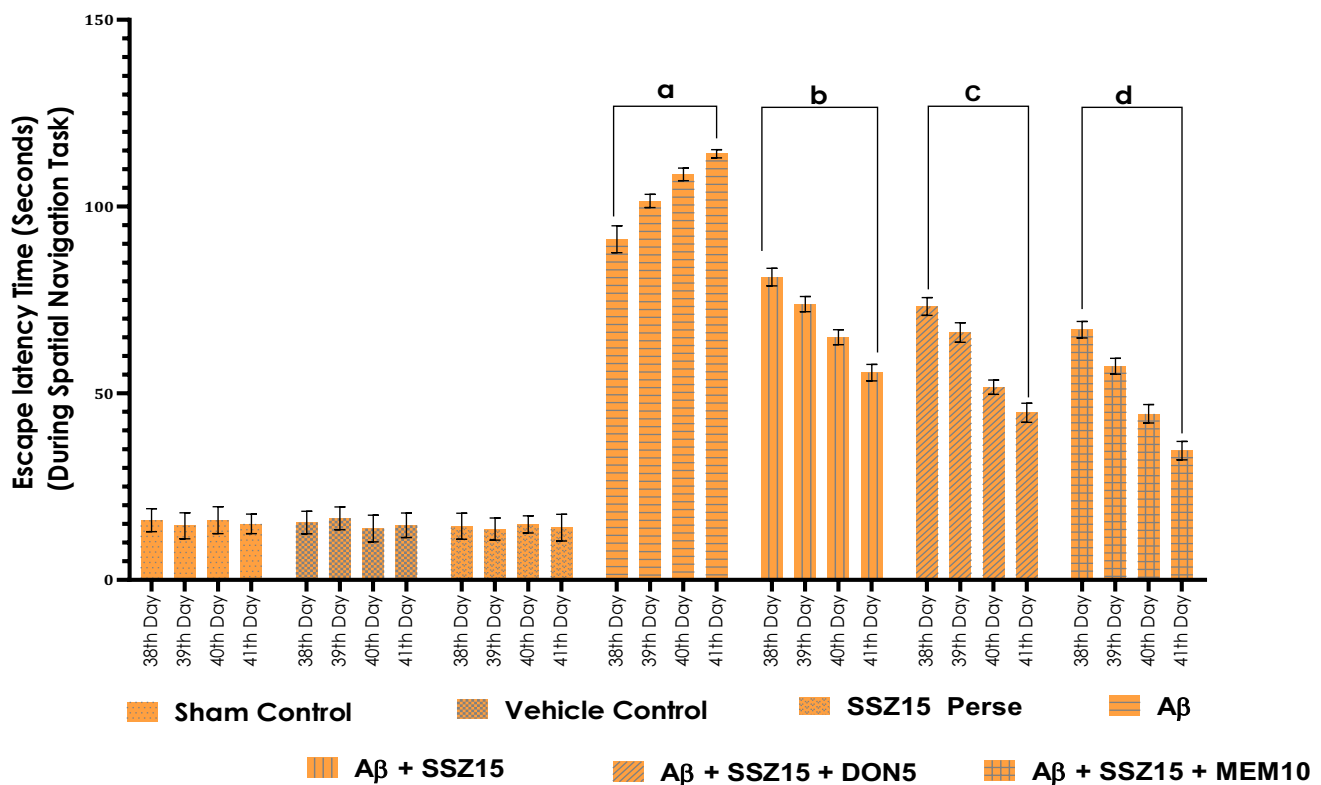
Fig. 5 Effect of SSZ compound on memory in Aβ-induced Alzheimer's rats. The statistical assessment used a two-way ANOVA and post hoc Bonferroni testing to analyze the data. Results are represented as mean values with standard deviation ($p < 0.05$), with each experimental group comprising eight Wistar rats. Statistical comparisons were made between groups: (**a**) versus sham control, vehicle control, and SSZ15 perse; (**b**) versus Aβ; (**c**) versus Aβ and SSZ15; and (**d**) versus Aβ, SSZ15, and DON5

isolating the cortex, striatum, and hippocampus. Within the sham control group, normal cortical, hippocampal, and striatal brain tissues were identified using green, red, and blue markers, respectively. Similar tissue presentations were observed in both the vehicle control and SSZ perse groups.

Conversely, the Aβ-induced (D) group displayed evident tissue degradation and a reduced appearance in the lower panel sections. However, with the continuous administration of SSZ at 15 mg/kg for 21 days, normal cortex, striatum, and hippocampus tissue morphology was restored. Subsequent administration of Aβ alongside SSZ15 and DON5 (F) notably exacerbated the degradation of hippocampal and striatal brain tissues, as indicated by marked yellow areas. Notably, treatment with SSZ at 15 mg/kg in combination with Aβ and MEM at 10 mg/kg showed improved tissue morphology and reduced tissue destruction. This underscores the significant brain tissue preservation and restoration attributed to SSZ at 15 mg/kg, countering the damage induced by Aβ and MEM10 (scale = 5 mm) (Fig. 7).

Effect of SSZ Compound on Gross Morphological Dysfunctions (Midbrain Sections) in Aβ-Induced Alzheimer's Rats

Following a 42-day experimental protocol, all mature Wistar rats were euthanized. Their entire brains, freshly isolated and dissected, underwent the removal of coronal sections, focusing on the midbrain region. In the sham control group, normal midbrain tissue was marked with a black circle, exhibiting characteristics consistent with the vehicle control and SSZ perse groups. However, the Aβ (D) group's midbrain sections displayed noticeable reductions in white matter fibers, substantial damage, and a shrunken appearance. The Aβ and SSZ (15 mg/kg) (E) group showed decreased damage severity in marked midbrain sections. Conversely, the Aβ, DON5, and SSZ (15 mg/kg) (F) groups exhibited a dose-dependent reduction in Aβ-induced damage. SSZ at this dosage restored normal midbrain tissue morphology and revived white matter fibers. Furthermore, in the Aβ, MEM (10 mg/kg), and SSZ (15 mg/kg) (G) groups, SSZ treatment at 15 mg/kg demonstrated reduced tissue degradation and
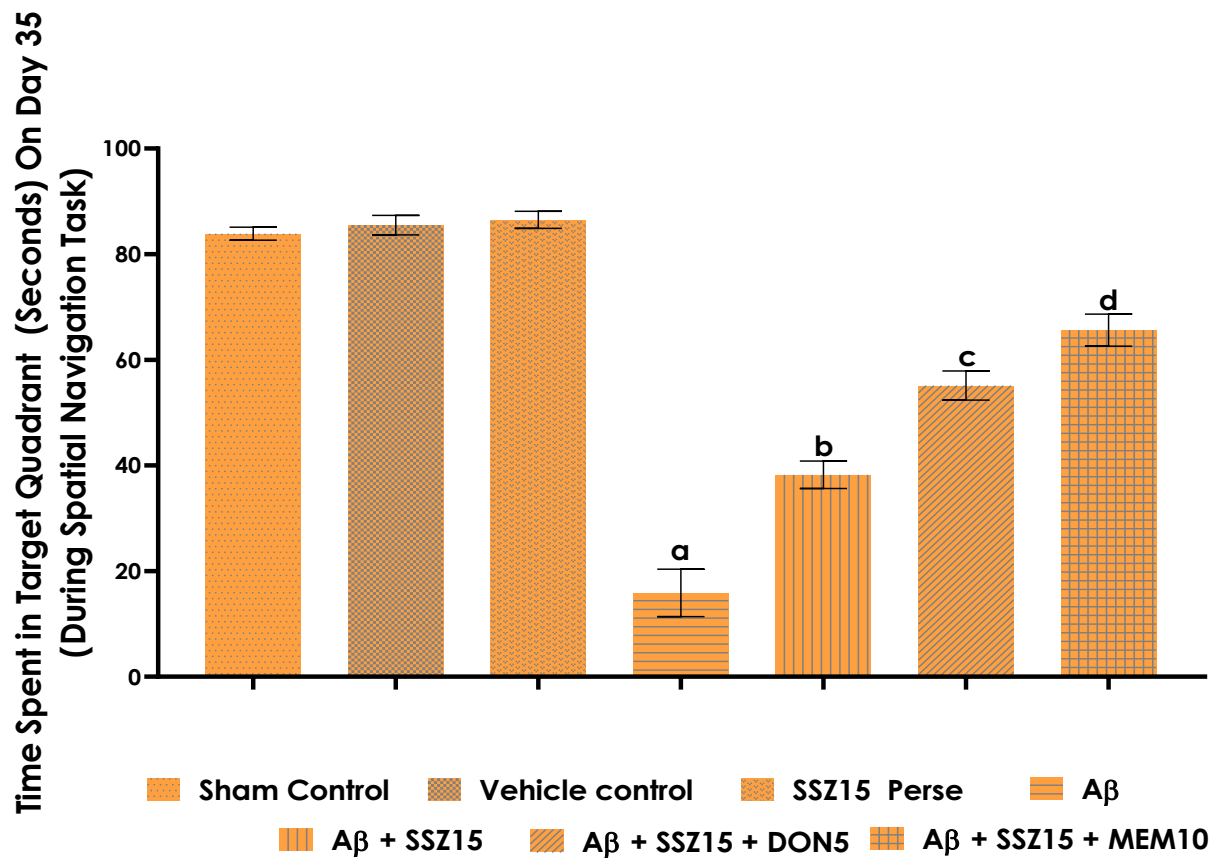
Fig. 6 Effect of SSZ compound on TSTQ in Aβ-induced Alzheimer's rats. The statistical assessment used a one-way ANOVA and post hoc Tuckey's testing to analyze the data. Results are represented as mean values with standard deviation ($p < 0.05$), with each experimental group comprising eight Wistar rats. Statistical comparisons were made between groups: (**a**) versus sham control, vehicle control, and SSZ15 perse; (**b**) versus Aβ; (**c**) versus Aβ and SSZ15; and (**d**) versus Aβ, SSZ15, and DON5

improved tissue structure. These findings illustrate that a 15 mg/kg dose of SSZ significantly mitigates brain tissue destruction caused by Aβ induction, facilitating tissue recovery (scale = 5 mm) (Fig. 8).

Discussion

Alzheimer's disease (AD) is a neurological condition characterized by memory loss, communication challenges, and spatial disorientation [4]. Due to the present treatment regimen's limited success and high costs, targeting multiple enzymes has been the research focus lately. The enzymes that are being explored are acetylcholinesterase, butyrylcholinesterase, glycogen synthase kinase 3, BACE-1, gamma-secretase, etc. [18–20, 58]. We have pursued this research for years to develop a viable multitargeted medicament for treating AD. Our research group completed a comprehensive in silico screening and reported some potential lead compounds that could target multiple enzymes, viz. acetylcholinesterase, butyrylcholinesterase, glycogen synthase kinase 3, BACE-1,

and gamma-secretase, and possibly provide a successful anti-AD drug [18–20]. We utilized a comprehensive computational approach using various in silico methods to screen and identify lead compounds targeting multiple enzymes implicated in AD pathophysiology. By taking advantage of molecular docking, we used virtual screening algorithms to shift through large libraries of chemical compounds and identified those with structural features likely to interact favorably with the target enzymes. A total of 13 ligands (BRW, 6VK, 6Z5, SMH, X37, 55E, 65 A, IQ6, 6VL, 6VM, F1B, 6Z2, and GVP) were selected based on blood–brain barrier (BBB) permeability, acceptable ADME properties as well as their molecular interaction profiles with the target enzymes [20]. Among the 13 ligands, eight ligands (55E, 6Z2, 6Z5, BRW, F1B, GVP, IQ6, and X37) showed binding energies of ≤ −8.0 kcal/mol towards BChE, BACE-1, and gamma-secretase MAO-A and MAO-B and formed a stable complex with target enzymes. After critical evaluation of resources, ease of synthesis, cost-effectiveness, and inherent pharmacophoric features of anti-AD drugs, we chose to synthesize IQ6 (SSZ).
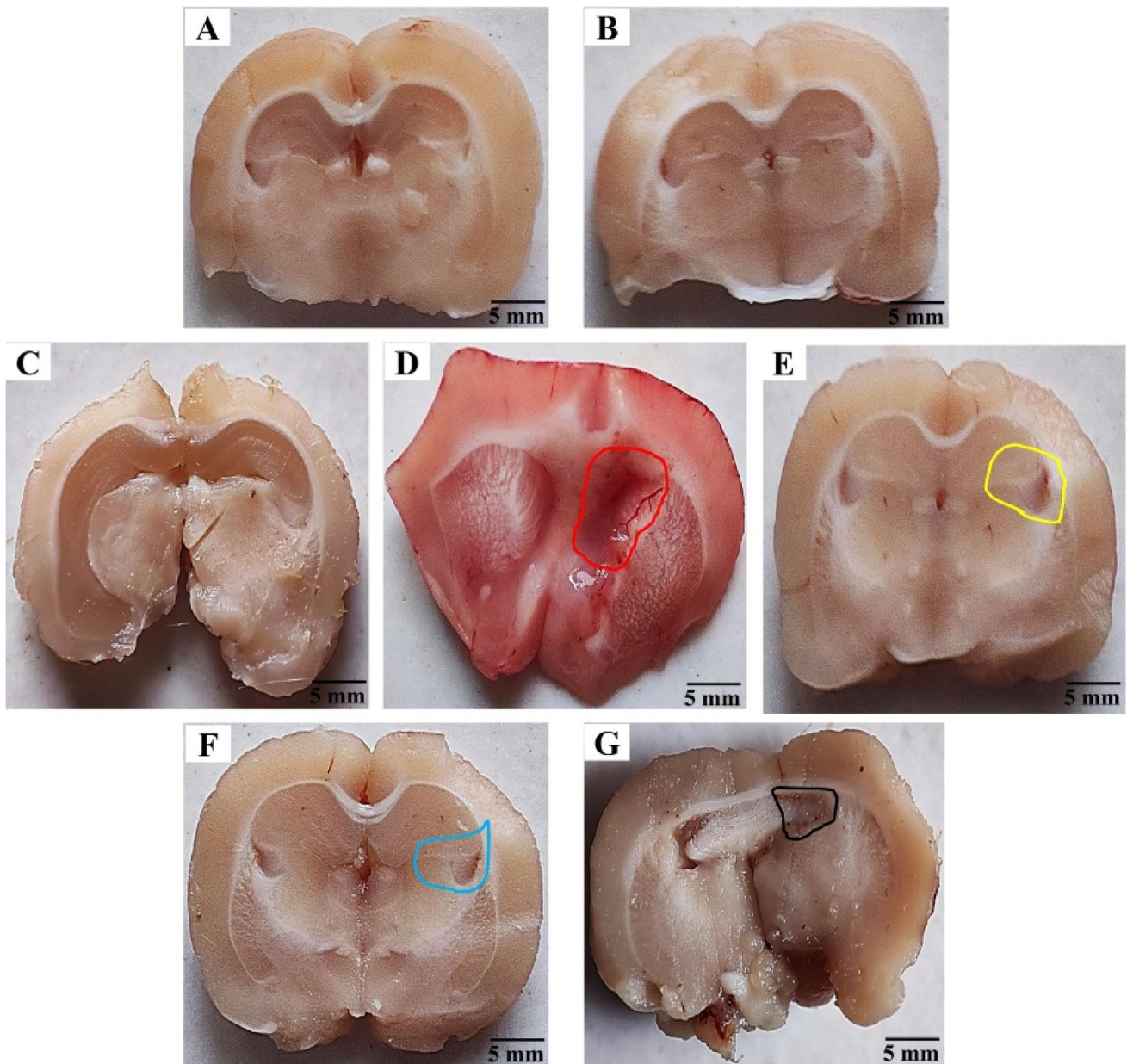
Fig. 7 Effect of SSZ compound on gross morphological dysfunctions (coronal sections) in Aβ-induced Alzheimer's rats. (**A**) Sham control. (**B**) Vehicle control. (**C**) SSZ perse. (**D**) Aβ. (**E**) Aβ + SSZ15. (**F**) Aβ + SSZ15 + DON5. (**G**) EB + SSZ15 + MEM15. On the 43rd day of the experiment, Wistar rats were euthanized for brain analysis. Sections of the cortex, striatum, and hippocampus were carefully extracted from fresh brain samples. The experimental groups, namely sham control (**A**), vehicle control (**B**), and SSZ perse (**C**), exhibited normal brain areas in the cortex, hippocampus, and striatum. However, the Aβ group (**D**) displayed signs of tissue degeneration. Notably, the degradation caused by Aβ decreased dose-dependently following 21 days of continuous SSZ therapy. Moreover, Aβ in combination with SSZ (15 mg/kg) (**E**) led to the destruction of cortical, hippocampal, and striatal brain tissues. Conversely, the combination of Aβ, DON (5 mg/kg), and SSZ (15 mg/kg) (**F**) improved tissue structure and reduced damage. Additionally, the standard drug MEM (10 mg/kg) dosage mitigated brain tissue degradation caused by Aβ and facilitated repair of the tissue layers affected by its impact

SSZ (IQ6) is a chemical molecule with the molecular structure of 6-chloro-N-cyclohexyl-4-(1H-pyrrolo [2,3-b] pyridin-3-yl) pyridin-2-amine. It contains pyrrolopyridine and N-cyclohexyl groups and demonstrated significant anti-Alzheimer properties [22]. Pyrrolopyridines have long-standing pharmacological activities, including antiviral, anticancer, and antibacterial properties. They also serve as a structural moiety in anti-AD therapeutic targets like phosphodiesterase and monoamine oxidase B. In addition, N-cyclohexyl fragments are commonly used
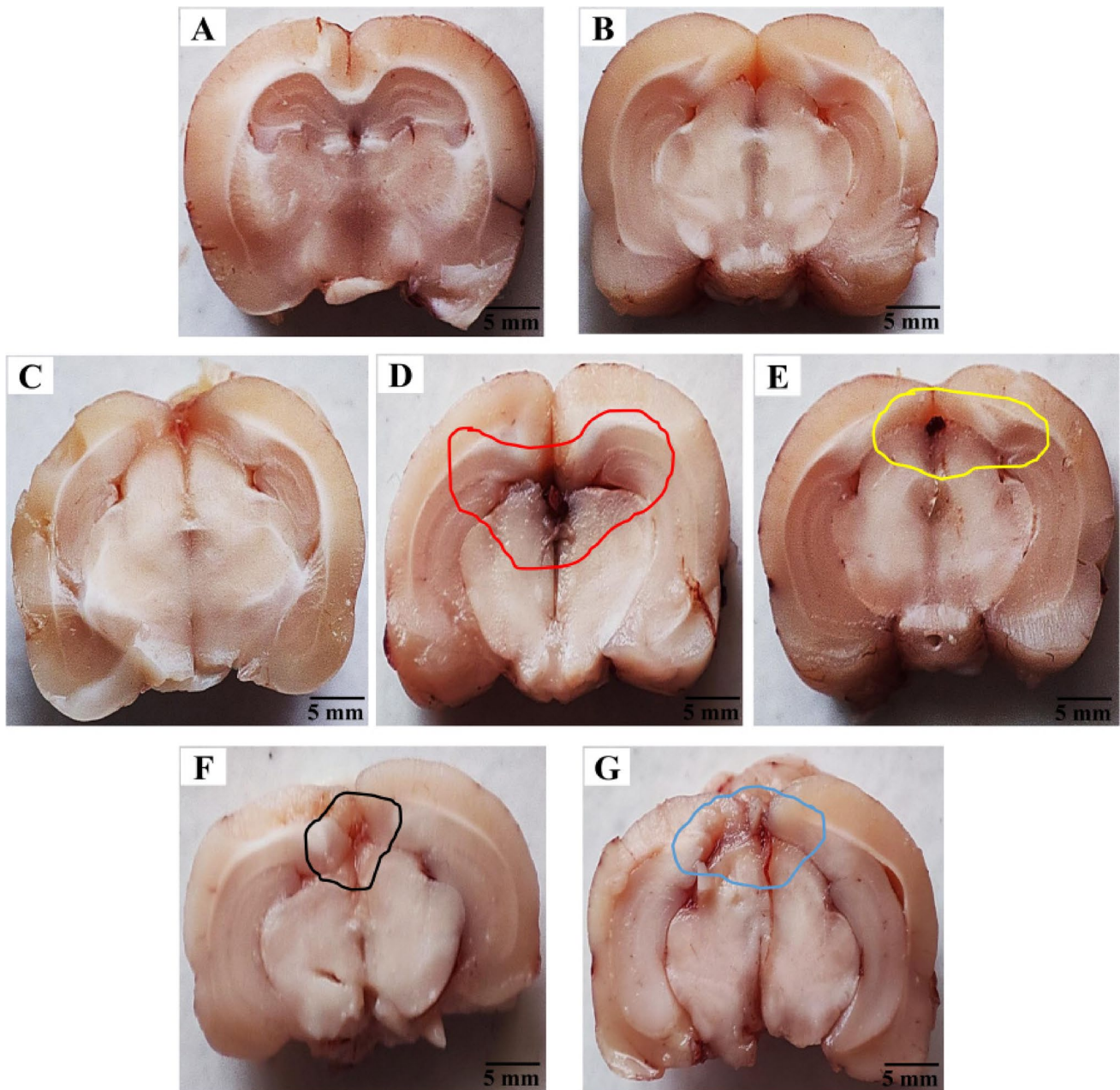
Fig. 8 Effect of SSZ compound on gross morphological dysfunctions (midbrain sections) in Aβ-induced Alzheimer's rats. (**A**) Sham control. (**B**) Vehicle control. (**C**) SSZ perse. (**D**) Aβ. (**E**) Aβ+SSZ15. (**F**) Aβ+SSZ15+DON5. (**G**) EB+SSZ15+MEM15. On the 43rd day of the experiment, Wistar rats were euthanized for analysis. Their brains were promptly extracted, with a distinction made between coronal and midbrain sections. Among the experimental groups—sham control (**A**), vehicle control (**B**), and SSZ perse (**C**) normal morphological features were observed. However, the Aβ (**D**) group displayed decreased white matter fibers, significant damage, and a contracted appearance. Treatment with SSZ at a dosage of 15 mg/kg restored the midbrain and white matter filaments to a normal state. Conversely, Aβ, SSZ (15 mg/kg), and DON5 (**F**) exacerbated tissue damage. Aβ, MEM (10 mg/kg), and SSZ (15 mg/kg) (**G**) resulted in improved tissue structure and decreased degeneration. Notably, SSZ (15 mg/kg) demonstrated reduced brain tissue loss and remediation of damage caused by Aβ

in natural and manufactured medications as a side chain or structural component and have been shown inhibitory activities against targets like butyrylcholinesterase and BACE1 [21, 26–30]. Moreover, N-cyclohexyl group is hydrophobic and attracts the protein's hydrophobic region and enhances hydrophobic interaction with the protein. The lipophilicity of N-cyclohexyl facilitates crossing the blood–brain barrier. It has conformational stability and prevents the protein from adopting unstable conformation [59, 60].

Earlier studies suggested the considerable involvement of Aβ (1–42) in the development of AD [32, 34, 61]. The main pathological characteristic of AD is the accumulation of Aβ peptides in the hippocampus and frontal cortex, which affect the production, clearance rate, and metabolic pathways [62]. In our study, we induced AD in rats by injecting ICV with Aβ (1–42) and subsequently conducted different behavioral tests, including LA, neuromuscular coordination, and spatial learning and memory tests. Early studies demonstrated that individuals with mild and severe AD exhibit impairments in essential functional abilities, such as walking, turning, sitting, sitting to stand, response time, and cognitive functions [63, 64]. In a preclinical study, the group of rats with AD demonstrated decreased locomotor activity on the actophotometer compared to the healthy group. Continued treatment with medications like baicalein and memantine led to significant progress in restoring locomotion [65, 66]. In the present work, LA decreased in Aβ (1–42)-treated rats but improved after SSZ treatment. The transgenic mice administered with Aβ exhibited deficits in their performance on the balance beam compared to non-transgenic controls [67]. Our work demonstrated that persistent delivery of Aβ (1–42) to rats resulted in gait abnormalities, which were found to be significantly recovered in response to SSZ treatment.

Recent studies demonstrated that the accumulation of soluble and insoluble Aβ aggregates in the brain contributes to cognitive and memory decline in AD individuals [68]. In a preclinical investigation, AD mice showed significantly impaired cognitive function in the MWM test, as evidenced by increased ELT and decreased TSTQ values [69]. We also found a significant memory loss, indicated by increased ELT and reduced time in the TSTQ. However, administering SSZ (15 mg/kg) enhanced cognition and long-term memory, and decreased ELT compared to the normal control group. The relationship between more significant weight loss and deteriorating neuroinflammation in Tg mice suggests that Aβ pathology might contribute to adverse outcomes following a systemic inflammatory challenge [70]. In our investigation, rats consistently administered with Aβ (1–42) exhibited decreased body weight compared to the sham, control, and perse groups. Additionally, administering SSZ in combination with conventional drugs, such as DON and MEM, resulted in a notable increase in body weight compared to rats receiving Aβ (1–42) only.

Clinical examination of 47 AD brains revealed Aβ deposits in the neocortex, all cortical brain regions, striatum, diencephalic nuclei, and basal forebrain. In phase 3, brainstem nuclei get involved, and in phase 4, cerebellar Aβ deposits are seen. According to Thal et al. [71], 17 AD patients with clinical confirmation include Aβ stages 3–5 [71]. Aβ1–42

injection in rats leads to hippocampus neuronal loss and apoptosis, resulting in cognitive impairment and elevated levels of APP. The alterations are associated with T-cell and glial-mediated neuroinflammation [72]. We analyzed the morphological alterations in the coronal sections and mid-brain areas of rats treated with Aβ (1–42) and found notable lesions. However, the continuous administration of SSZ led to enhanced morphological improvements, decreasing the lesion volume in coronal sections. The novel SSZ compound protected oval neurons with spherical nuclei and oligodendrocytes against Aβ-induced damage. Rats administered with Aβ exhibited atypical morphology in distinct brain regions [46, 52, 73, 74]. SSZ, DON, and MEM treatment significantly improved these morphologies, showing neuroprotective effects. Additional research is required to comprehend the exact influence of Aβ on the deformation of the coronal and midbrain regions.

The treatment of SSZ in AD rats significantly reduced the impacts of AD on behavioral measures, including locomotor activity, neuromuscular coordination, spatial memory, and body weight alterations. SSZ also improved neuroprotection in brain tissues, particularly coronal and midbrain slices, by reducing tissue damage and maintaining neuronal and oligodendrocyte morphology. It was expected, considering the possible mechanisms of action of a compound with a chemical structure that includes pyrrolopyridine and N-cyclohexyl groups, which target specific pathways and enzymes associated with AD, such as neuroinflammation, synaptic dysfunction, and Aβ aggregation [21, 25, 28, 30]. Another important aspect of the current study was the combination of SSZ with conventional drugs like DON and MEM, which was found to effectively mitigate cognitive impairments and morphological lesions induced by Aβ (1–42) injection in rats. The combination therapy also showed greater improvements in memory consolidation and cognitive function compared to individual treatments. The synergistic effects observed in our study suggest that such combination treatments can address the multifactorial nature of AD more effectively than monotherapies.

Limitations

The focus of the current study was to synthesize a potent ligand molecule previously predicted for its potential anti-AD benefits through computational methods. However, over the molecular synthesis of ligand SSZ, the scope of the current study extends to its behavioral and cognitive effects using the Wistar rats AD model. Experimental validation of changes in molecular markers associated with AD mechanism after the treatment with SSZ is an additional value for its applicability as a possible anti-AD drug. We

have planned more systematic experimental evaluations and deep mechanistic observations in our future experimental work. Replicating the similar results in the human system is essential to ascertain SSZ suitability as a viable treatment option for AD. Future research should aim to incorporate a variety of approaches, including clinical studies with human subjects, to provide a more comprehensive understanding of the complex mechanism before considering this potent ligand from bench to bedside.

Conclusion

The current research presents compelling evidence for the potential efficacy of the synthesized compound SSZ in combating AD. The work underscores the necessity for novel therapeutic approaches that target multiple pathological pathways simultaneously. The conclusion drawn from the study indicates promising outcomes of SSZ treatment in AD rat model, showcasing improvements in behavioral, cognitive, and neuroprotective parameters. SSZ, synthesized as a multitargeted ligand, demonstrated synergistic effects when combined with conventional drugs, suggesting a potential therapeutic strategy for AD management. Furthermore, SSZ's chemical structure incorporates pharmacologically active pyrrolopyridine and N-cyclohexyl groups known for their anti-AD effects, potentially enhancing its therapeutic properties. Overall, the study highlights the efficacy of multitargeted ligands like SSZ in addressing the complex etiology of AD. Further research is warranted to fully elucidate SSZ's therapeutic potential in clinical settings, offering hope for an effective AD treatment. This research represents a significant step towards developing a novel multitargeted therapeutic strategy for combating AD, which is crucial considering the increasing prevalence of the disease globally.

Declarations

Ethics Approval Not applicable.

Consent to Participate Not applicable.

Consent to Publish All authors have given their consent to publish this article.

Competing Interests The authors declare no competing interests.

References

1. Gustavsson A, Norton N, Fast T, Frölich L, Georges J, Holzapfel D, Kirabali T, Krolak-Salmon P et al (2023) Global estimates on the number of persons across the Alzheimer's disease continuum. Alzheimers Dement 19(2):658–670. https://doi.org/10.1002/alz.12694
2. Li X, Feng X, Sun X, Hou N, Han F, Liu Y (2022) Global, regional, and national burden of Alzheimer's disease and other dementias, 1990–2019. Front Aging Neurosci 14. https://doi.org/10.3389/fnagi.2022.937486
3. Jabir NR, Khan FR, Tabrez S (2018) Cholinesterase targeting by polyphenols: a therapeutic approach for the treatment of Alzheimer's disease. CNS Neurosci Ther 24(9):753–762. https://doi.org/10.1111/cns.12971
4. Hoque M, Samanta A, Alam SSM, Zughaibi TA, Kamal MA, Tabrez S (2023) Nanomedicine-based immunotherapy for Alzheimer's disease. Neurosci Biobehav Rev 144:104973. https://doi.org/10.1016/j.neubiorev.2022.104973
5. Makhaeva GF, Lushchekina SV, Kovaleva NV, Yu Astakhova T, Boltneva NP, Rudakova EV, Serebryakova OG, Proshin AN et al (2021) Amiridine-piperazine hybrids as cholinesterase inhibitors and potential multitarget agents for Alzheimer's disease treatment. Bioorg Chem 112:104974. https://doi.org/10.1016/j.bioorg.2021.104974
6. Islam BU, Jabir NR, Tabrez S (2019) The role of mitochondrial defects and oxidative stress in Alzheimer's disease. J Drug Target 27(9):932–942. https://doi.org/10.1080/1061186X.2019.1584808
7. Rai SN, Singh C, Singh A, Singh MP, Singh BK (2020) Mitochondrial dysfunction: a potential therapeutic target to treat Alzheimer's disease. Mol Neurobiol 57(7):3075–3088. https://doi.org/10.1007/s12035-020-01945-y
8. Rai SN, Zahra W, Birla H, Singh SS, Singh SP (2018) Mild endoplasmic reticulum stress ameliorates lpopolysaccharide-induced neuroinflammation and cognitive impairment via regulation of microglial polarization. Front Aging Neurosci 10:192. https://doi.org/10.3389/fnagi.2018.00192
9. Tripathi PN, Srivastava P, Sharma P, Tripathi MK, Seth A, Tripathi A, Rai SN, Singh SP et al (2019) Biphenyl-3-oxo-1,2,4-triazine linked piperazine derivatives as potential cholinesterase inhibitors with antioxidant property to improve the learning and memory. Bioorg Chem 85:82–96. https://doi.org/10.1016/j.bioorg.2018.12.017
10. Singh M, Kaur M, Vyas B, Silakari O (2018) Design, synthesis and biological evaluation of 2-Phenyl-4H-chromen-4-one derivatives as polyfunctional compounds against Alzheimer's disease. Med Chem Res 27(2):520–530. https://doi.org/10.1007/s00044-017-2078-4
11. Srivastava P, Tripathi PN, Sharma P, Rai SN, Singh SP, Srivastava RK, Shankar S, Shrivastava SK (2019) Design and development of some phenyl benzoxazole derivatives as a potent acetylcholinesterase inhibitor with antioxidant property to enhance learning and memory. Eur J Med Chem 163:116–135. https://doi.org/10.1016/j.ejmech.2018.11.049

12. Zhang N, Gan L, Xiang G, Xu J, Jiang T, Li Y, Wu Y, Ni R et al (2024) Cholinesterase inhibitors-associated torsade de pointes/QT prolongation: a real-world pharmacovigilance study. Front Pharmacol 14. https://doi.org/10.3389/fphar.2023.1343650

13. Obrenovich M, Tabrez S, Siddiqui B, McCloskey B, Perry G (2020) The microbiota-gut-brain axis-heart shunt part II: prosaic foods and the brain-heart connection in Alzheimer disease. Microorganisms 8(4):493. https://doi.org/10.3390/microorganisms8040493

14. Long J, Qin F, Luo J, Zhong G, Huang S, Jing L, Yi T, Liu J et al (2024) Design, synthesis, and biological evaluation of novel capsaicin-tacrine hybrids as multi-target agents for the treatment of Alzheimer's disease. Bioorg Chem 143:107026. https://doi.org/10.1016/j.bioorg.2023.107026

15. Drakontaeidi A, Pontiki E (2024) Multi-target-directed cinnamic acid hybrids targeting Alzheimer's disease. Int J Mol Sci 25(1):582. https://doi.org/10.3390/ijms25010582

16. Hafez DE, Dubiel M, La Spada G, Catto M, Reiner-Link D, Syu Y-T, Abdel-Halim M, Hwang T-L et al (2023) Novel benzothiazole derivatives as multitargeted-directed ligands for the treatment of Alzheimer's disease. J Enzyme Inhib Med Chem 38(1):2175821. https://doi.org/10.1080/14756366.2023.2175821

17. Jabir NR, Rehman MT, AlAjmi MF, Ahmed BA, Tabrez S (2023) Prioritization of bioactive compounds envisaging yohimbine as a multi targeted anticancer agent: insight from molecular docking and molecular dynamics simulation. J Biomol Struct Dyn 41(20):10463–10477. https://doi.org/10.1080/07391102.2022.2158137

18. Jabir NR, Rehman MT, Alsolami K, Shakil S, Zughaibi TA, Alserihi RF, Khan MS, AlAjmi MF et al (2021) Concatenation of molecular docking and molecular simulation of BACE-1, γ-secretase targeted ligands: in pursuit of Alzheimer's treatment. Ann Med 53(1):2332–2344. https://doi.org/10.1080/07853890.2021.2009124

19. Jabir NR, Rehman MT, Tabrez S, Alserihi RF, AlAjmi MF, Khan MS, Husain FM, Ahmed BA (2021) Identification of butyrylcholinesterase and monoamine oxidase B targeted ligands and their putative application in Alzheimer's treatment: a computational strategy. Curr Pharm Des 27(20):2425–2434. https://doi.org/10.2174/1381612827666210226123240

20. Jabir NR, Shakil S, Tabrez S, Khan MS, Rehman MT, Ahmed BA (2021) In silico screening of glycogen synthase kinase-3β targeted ligands against acetylcholinesterase and its probable relevance to Alzheimer's disease. J Biomol Struct Dyn 39(14):5083–5092. https://doi.org/10.1080/07391102.2020.1784796

21. Haghighijoo Z, Akrami S, Saeedi M, Zonouzi A, Iraji A, Larijani B, Fakherzadeh H, Sharifi F et al (2020) N-Cyclohexylimidazo[1,2-a]pyridine derivatives as multi-target-directed ligands for treatment of Alzheimer's disease. Bioorg Chem 103:104146. https://doi.org/10.1016/j.bioorg.2020.104146

22. Konecny J, Misiachna A, Hrabinova M, Pulkrabkova L, Benkova M, Prchal L, Kucera T, Kobrlova T et al (2020) Pursuing the complexity of Alzheimer's disease: discovery of fluoren-9-amines as selective butyrylcholinesterase inhibitors and N-methyl-d-aspartate receptor antagonists. Biomolecules 11(1):3. https://doi.org/10.3390/biom11010003

23. Dorababu A (2022) Promising heterocycle-based scaffolds in recent (2019–2021) anti-Alzheimer's drug design and discovery. Eur J Pharmacol 920:174847. https://doi.org/10.1016/j.ejphar.2022.174847

24. Wójcicka A, Redzicka A (2021) An overview of the biological activity of pyrrolo[3,4-c]pyridine derivatives. Pharmaceuticals (Basel) 14(4):354. https://doi.org/10.3390/ph14040354

25. Jeelan Basha N, Basavarajaiah SM, Shyamsunder K (2022) Therapeutic potential of pyrrole and pyrrolidine analogs: an update. Mol Divers 26(5):2915–2937. https://doi.org/10.1007/s11030-022-10387-8

26. Istanbullu H, Bayraktar G, Saylam M, Istanbullu H, Bayraktar G, Saylam M (2022) Fused pyridine derivatives: synthesis and biological activities. In: Exploring chemistry with pyridine derivatives. IntechOpen. https://doi.org/10.5772/intechopen.107537

27. Bianco MdCAD, Marinho DILF, Hoelz LVB, Bastos MM, Boechat N (2021) Pyrroles as privileged scaffolds in the search for new potential HIV inhibitors. Pharmaceuticals (Basel) 14(9):893. https://doi.org/10.3390/ph14090893

28. Saigal GYSA, Uddin A, Khan S, Abid M, Khan MM (2021) Synthesis, biological evaluation and docking studies of functionalized pyrrolo[3,4-b]pyridine derivatives. ChemistrySelect 6(9):2323–2334. https://doi.org/10.1002/slct.202004781

29. Vadukoot AK, Sharma S, Aretz CD, Kumar S, Gautam N, Alnouti Y, Aldrich AL, Heim CE et al (2020) Synthesis and SAR studies of 1H-pyrrolo[2,3-b]pyridine-2-carboxamides as phosphodiesterase 4B (PDE4B) inhibitors. ACS Med Chem Lett 11(10):1848–1854. https://doi.org/10.1021/acsmedchemlett.9b00369

30. Tzvetkov NT, Stammler H-G, Hristova S, Atanasov AG, Antonov L (2019) (Pyrrolo-pyridin-5-yl)benzamides: BBB permeable monoamine oxidase B inhibitors with neuroprotective effect on cortical neurons. Eur J Med Chem 162:793–809. https://doi.org/10.1016/j.ejmech.2018.11.009

31. Tong Y, Stewart KD, Florjancic AS, Harlan JE, Merta PJ, Przytulinska M, Soni N, Swinger KK et al (2013) Azaindole-based inhibitors of Cdc7 kinase: impact of the Pre-DFG residue, Val 195. ACS Med Chem Lett 4(2):211–215. https://doi.org/10.1021/ml300348c

32. Guzmán-Ruiz MA, Herrera-González A, Jiménez A, Candelas-Juárez A, Quiroga-Lozano C, Castillo-Díaz C, Orta-Salazar E, Organista-Juárez D et al (2021) Protective effects of intracerebroventricular adiponectin against olfactory impairments in an amyloid β1-42 rat model. BMC Neurosci 22(1):14. https://doi.org/10.1186/s12868-021-00620-9

33. Sharma S, Verma S, Kapoor M, Saini A, Nehru B (2016) Alzheimer's disease like pathology induced six weeks after aggregated amyloid-beta injection in rats: increased oxidative stress and impaired long-term memory with anxiety-like behavior. Neurol Res 38(9):838–850. https://doi.org/10.1080/01616412.2016.1209337

34. Cetin F, Yazihan N, Dincer S, Akbulut G (2013) The effect of intracerebroventricular injection of beta amyloid peptide (1–42) on caspase-3 activity, lipid peroxidation, nitric oxide and NOS expression in young adult and aged rat brain. Turk Neurosurg 23(2):144–150. https://doi.org/10.5137/1019-5149.JTN.5855-12.1

35. Guo J, Wang Z, Liu R, Huang Y, Zhang N, Zhang R (2020) Memantine, donepezil, or combination therapy-what is the best therapy for Alzheimer's disease? A network meta-analysis Brain Behav 10(11):e01831. https://doi.org/10.1002/brb3.1831

36. Anoush M, Bijani S, Moslemifar F, Jahanpour F, Kalantari-Hesari A, Hosseini M-J (2023) Edaravone improves streptozotocin-induced memory impairment via alleviation of behavioral dysfunction, oxidative stress, inflammation, and histopathological parameters. Behav Neurol 2023:e9652513. https://doi.org/10.1155/2023/9652513

37. Zhang Y, Chen H, Li R, Sterling K, Song W (2023) Amyloid β-based therapy for Alzheimer's disease: challenges, successes and future. Signal Transduct Target Ther 8(1):248. https://doi.org/10.1038/s41392-023-01484-7

38. Chhabra S, Mehan S, Khan Z, Gupta GD, Narula AS (2023) Matrine mediated neuroprotective potential in experimental multiple sclerosis: evidence from CSF, blood markers, brain samples and in-silico investigations. J Neuroimmunol 384. https://doi.org/10.1016/j.jneuroim.2023.578200

39. Kumar A, Lana E, Kumar R, Lithner CU, Darreh-Shori T (2018) P1–241: soluble amyloid-beta activates choline acetyltransferase.

Alzheimer's & Dementia 14 (7S_Part_7):P371-P371. https://doi.org/10.1016/j.jalz.2018.06.246

40. Alkandari AF, Madhyastha S, Rao MS (2023) N-Acetylcysteine amide against Aβ-induced Alzheimer's-like pathology in rats. Int J Mol Sci 24(16):12733. https://doi.org/10.3390/ijms241612733

41. Sethi P, Mehan S, Khan Z, Chhabra S (2023) Acetyl-11-keto-beta boswellic acid(AKBA) modulates CSTC-pathway by activating SIRT-1/Nrf2-HO-1 signalling in experimental rat model of obsessive-compulsive disorder: evidenced by CSF, blood plasma and histopathological alterations. Neurotoxicology 98:61–85. https://doi.org/10.1016/j.neuro.2023.08.001

42. Alharbi M, Alshammari A, Kaur G, Kalra S, Mehan S, Suri M, Chhabra S, Kumar N et al (2022) Effect of natural adenylcyclase/cAMP/CREB signalling activator forskolin against intra-striatal 6-OHDA-lesioned Parkinson's rats: preventing mitochondrial, motor and histopathological defects. Molecules 27(22):7951. https://doi.org/10.3390/molecules27227951

43. Khera R, Mehan S, Bhalla S, Kumar S, Alshammari A, Alharbi M, Sadhu SS (2022) Guggulsterone mediated JAK/STAT and PPAR-gamma modulation prevents neurobehavioral and neurochemical abnormalities in propionic acid-induced experimental model of autism. Molecules (Basel, Switzerland) 27(3):889. https://doi.org/10.3390/molecules27030889

44. Singh A, Upadhayay S, Mehan S (2021) Inhibition of c-JNK/p38MAPK signaling pathway by Apigenin prevents neurobehavioral and neurochemical defects in ethidium bromide-induced experimental model of multiple sclerosis in rats: evidence from CSF, blood plasma and brain samples. Phytomed Plus 1(4):100139. https://doi.org/10.1016/j.phyplu.2021.100139

45. Duggal P, Jadaun KS, Siqqiqui EM, Mehan S (2020) Investigation of low dose cabazitaxel potential as microtubule stabilizer in experimental model of Alzheimer's disease: restoring neuronal cytoskeleton. Curr Alzheimer Res 17(7):601–615. https://doi.org/10.2174/1567205017666201007120112

46. Bhalla S, Mehan S (2022) 4-Hydroxyisoleucine mediated IGF-1/GLP-1 signalling activation prevents propionic acid-induced autism-like behavioural phenotypes and neurochemical defects in experimental rats. Neuropeptides 96:102296. https://doi.org/10.1016/j.npep.2022.102296

47. Sharma A, Bhalla S, Mehan S (2022) PI3K/AKT/mTOR signalling inhibitor chrysophanol ameliorates neurobehavioural and neurochemical defects in propionic acid-induced experimental model of autism in adult rats. Metab Brain Dis 37(6):1909–1929. https://doi.org/10.1007/s11011-022-01026-0

48. Mehan S, Meena H, Sharma D, Sankhla R (2011) JNK: a stress-activated protein kinase therapeutic strategies and involvement in Alzheimer's and various neurodegenerative abnormalities. J Mol Neurosci 43(3):376–390. https://doi.org/10.1007/s12031-010-9454-6

49. Upadhayay S, Mehan S, Prajapati A, Sethi P, Suri M, Zawawi A, Almashjary MN, Tabrez S (2022) Nrf2/HO-1 signaling stimulation through acetyl-11-keto-beta-boswellic acid (AKBA) provides neuroprotection in ethidium bromide-induced experimental model of multiple sclerosis. Genes (Basel) 13(8):1324. https://doi.org/10.3390/genes13081324

50. Gupta R, Mehan S, Sethi P, Prajapati A, Alshammari A, Alharbi M, Al-Mazroua HA, Narula AS (2022) Smo-Shh agonist purmorphamine prevents neurobehavioral and neurochemical defects in 8-OH-DPAT-induced experimental model of obsessive-compulsive disorder. Brain Sci 12(3):342. https://doi.org/10.3390/brainsci12030342

51. Rahi S, Gupta R, Sharma A, Mehan S (2021) Smo-Shh signaling activator purmorphamine ameliorates neurobehavioral, molecular, and morphological alterations in an intracerebroventricular propionic acid-induced experimental model of autism. Hum Exp

Toxicol 40(11):1880–1898. https://doi.org/10.1177/0960327121013456

52. Prajapati A, Mehan S, Khan Z, Chhabra S, Das Gupta G (2023) Purmorphamine, a Smo-Shh/Gli activator, promotes sonic hedgehog-mediated neurogenesis and restores behavioural and neurochemical deficits in experimental model of multiple sclerosis. Neurochem Res. https://doi.org/10.1007/s11064-023-04082-9

53. Shandilya A, Mehan S, Kumar S, Sethi P, Narula AS, Alshammari A, Alharbi M, Alasmari AF (2022) Activation of IGF-1/GLP-1 Signalling via 4-hydroxyisoleucine prevents motor neuron impairments in experimental ALS-rats exposed to methylmercury-induced neurotoxicity. Molecules (Basel, Switzerland) 27(12):3878. https://doi.org/10.3390/molecules27123878

54. Sharma S, Mehan S, Khan Z, Gupta GD, Narula AS (2024) Icariin prevents methylmercury-induced experimental neurotoxicity: evidence from cerebrospinal fluid, blood plasma, brain samples, and in-silico investigations. Heliyon 10(1):e24050. https://doi.org/10.1016/j.heliyon.2024.e24050

55. Rajkhowa B, Mehan S, Sethi P, Prajapati A, Suri M, Kumar S, Bhalla S, Narula AS et al (2022) Activating SIRT-1 signalling with the mitochondrial-CoQ10 activator solanesol improves neurobehavioral and neurochemical defects in ouabain-induced experimental model of bipolar disorder. Pharmaceuticals (Basel, Switzerland) 15(8):959. https://doi.org/10.3390/ph15080959

56. Kumar S, Mehan S, Khan Z, Das Gupta G, Narula AS (2024) Guggulsterone selectively modulates STAT-3, mTOR, and PPAR-gamma signaling in a methylmercury-exposed experimental neurotoxicity: evidence from CSF, blood plasma, and brain samples. Mol Neurobiol. https://doi.org/10.1007/s12035-023-03902-x

57. Kumar N, Sharma N, Khera R, Gupta R, Mehan S (2021) Guggulsterone ameliorates ethidium bromide-induced experimental model of multiple sclerosis via restoration of behavioral, molecular, neurochemical and morphological alterations in rat brain. Metab Brain Dis 36(5):911–925. https://doi.org/10.1007/s11011-021-00691-x

58. Maramai S, Benchekroun M, Gabr MT, Yahiaoui S (2020) Multitarget therapeutic strategies for Alzheimer's disease: review on emerging target combinations. Biomed Res Int 2020:5120230. https://doi.org/10.1155/2020/5120230

59. Hughes JD, Blagg J, Price DA, Bailey S, Decrescenzo GA, Devraj RV, Ellsworth E, Fobian YM et al (2008) Physicochemical drug properties associated with in vivo toxicological outcomes. Bioorg Med Chem Lett 18(17):4872–4875. https://doi.org/10.1016/j.bmcl.2008.07.071

60. Banks WA (2016) From blood–brain barrier to blood–brain interface: new opportunities for CNS drug delivery. Nat Rev Drug Discov 15(4):275–292. https://doi.org/10.1038/nrd.2015.21

61. Lehmann S, Dumurgier J, Ayrignac X, Marelli C, Alcolea D, Ormaechea JF, Thouvenot E, Delaby C et al (2020) Cerebrospinal fluid A beta 1–40 peptides increase in Alzheimer's disease and are highly correlated with phospho-tau in control individuals. Alzheimers Res Ther 12(1):123. https://doi.org/10.1186/s13195-020-00696-1

62. Yoon S-S, AhnJo S-M (2012) Mechanisms of amyloid-β peptide clearance: potential therapeutic targets for Alzheimer's disease. Biomol Ther 20(3):245–255. https://doi.org/10.4062/biomolther.2012.20.3.245

63. Serra-Añó P, Pedrero-Sánchez JF, Hurtado-Abellán J, Inglés M, Espí-López GV, López-Pascual J (2019) Mobility assessment in people with Alzheimer disease using smartphone sensors. J Neuroeng Rehabil 16(1):103. https://doi.org/10.1186/s12984-019-0576-y

64. Hebert LE, Bienias JL, McCann JJ, Scherr PA, Wilson RS, Evans DA (2010) Upper and lower extremity motor performance and functional

impairment in Alzheimer's disease. Am J Alzheimers Dis Other Demen 25(5):425–431. https://doi.org/10.1177/1533317510367636

65. Jadhav R, Kulkarni YA (2023) The combination of baicalein and memantine reduces oxidative stress and protects against β-amyloid-induced Alzheimer's disease in rat model. Antioxidants 12(3):707. https://doi.org/10.3390/antiox12030707

66. Jin X, Liu M-Y, Zhang D-F, Zhong X, Du K, Qian P, Yao W-F, Gao H et al (2019) Baicalin mitigates cognitive impairment and protects neurons from microglia-mediated neuroinflammation via suppressing NLRP3 inflammasomes and TLR4/NF-κB signaling pathway. CNS Neurosci Ther 25(5):575–590. https://doi.org/10.1111/cns.13086

67. Arendash GW, King DL, Gordon MN, Morgan D, Hatcher JM, Hope CE, Diamond DM (2001) Progressive, age-related behavioral impairments in transgenic mice carrying both mutant amyloid precursor protein and presenilin-1 transgenes. Brain Res 891(1–2):42–53. https://doi.org/10.1016/s0006-8993(00)03186-3

68. van Dyck CH, Swanson CJ, Aisen P, Bateman RJ, Chen C, Gee M, Kanekiyo M, Li D et al (2023) Lecanemab in early Alzheimer's disease. N Engl J Med 388(1):9–21. https://doi.org/10.1056/NEJMoa2212948

69. Dhamodharan J, Sekhar G, Muthuraman A (2022) Epidermal growth factor receptor kinase inhibitor ameliorates β-amyloid oligomer-induced alzheimer disease in Swiss albino mice. Molecules 27(16):5182. https://doi.org/10.3390/molecules27165182

70. Knopp RC, Baumann KK, Wilson ML, Banks WA, Erickson MA (2022) Amyloid beta pathology exacerbates weight loss and brain cytokine responses following low-dose lipopolysaccharide in aged female Tg2576 mice. Int J Mol Sci 23(4):2377. https://doi.org/10.3390/ijms23042377

71. Thal DR, Rüb U, Orantes M, Braak H (2002) Phases of Aβ-deposition in the human brain and its relevance for the development of AD. Neurology 58(12):1791–1800. https://doi.org/10.1212/WNL.58.12.1791

72. Shen W-X, Chen J-H, Lu J-H, Peng Y-P, Qiu Y-H (2014) TGF-β1 protection against Aβ1–42-induced neuroinflammation and neurodegeneration in rats. Int J Mol Sci 15(12):22092–22108. https://doi.org/10.3390/ijms151222092

73. Jadaun KS, Sharma A, Siddiqui EM, Mehan S (2022) Targeting abnormal PI3K/AKT/mTOR signaling in intracerebral hemorrhage: a systematic review on potential drug targets and influences of signaling modulators on other neurological disorders. Curr Rev Clin Exp Pharmacol 17(3):174–191. https://doi.org/10.2174/1574884716666210726110021

74. Minj E, Upadhayay S, Mehan S (2021) Nrf2/HO-1 signaling activator acetyl-11-keto-beta boswellic acid (AKBA)-mediated neuroprotection in methyl mercury-induced experimental model of ALS. Neurochem Res 46(11):2867–2884. https://doi.org/10.1007/s11064-021-03366-2

Authors and Affiliations

Mohd Shahnawaz Khan[1] · Zuber Khan[2] · Nasimudeen R. Jabir[3] · Sidharth Mehan[2] · Mohd Suhail[4,5] · Syed Kashif Zaidi[6] · Torki A. Zughaibi[4,5] · Mohammad Abid[7] · Shams Tabrez[4,5]

✉ Sidharth Mehan
sidh.mehan@gmail.com

✉ Mohammad Abid
mabid@jmi.ac.in

✉ Shams Tabrez
shamstabrez1@gmail.com

Mohd Shahnawaz Khan
moskhan@ksu.edu.sa

Zuber Khan
zuber3491@gmail.com

Nasimudeen R. Jabir
jabirnr@gmail.com

Mohd Suhail
suhaildbt@gmail.com

Syed Kashif Zaidi
kashif_biochem@yahoo.com

Torki A. Zughaibi
taalzughaibi@kau.edu.sa

1   Department of Biochemistry, College of Science, King Saud University, Riyadh, Saudi Arabia

2   Department of Pharmacology, ISF College of Pharmacy (An Autonomous College), Moga 142001, Punjab, India

3   Department of Biochemistry, Centre for Research and Development, PRIST University, Vallam, Thanjavur, Tamil Nadu, India

4   King Fahd Medical Research Center, King Abdulaziz University, Jeddah, Saudi Arabia

5   Department of Medical Laboratory Sciences, Faculty of Applied Medical Sciences, King Abdulaziz University, Jeddah, Saudi Arabia

6   Center of Excellence in Genomic Medicine Research, King Abdulaziz University, Jeddah, Saudi Arabia

7   Medicinal Chemistry Laboratory, Department of Biosciences, Jamia Millia Islamia, New Delhi, India